J. Fluid Mech. (1973), *vol.* 57, *part* 4, *pp.* 695–719
Printed in Great Britain

A linearized potential flow theory for airfoils with spoilers

By G. P. BROWN AND G. V. PARKINSON
Department of Mechanical Engineering, University of British Columbia

(Received 14 August 1972)

Linearized two-dimensional potential flow theory is applied to an airfoil with an upper surface spoiler. The spoiler wake is modelled as a cavity of empirically given constant pressure, and a sequence of conformal transformations maps the linearized physical plane, with a slit on the real axis representing the airfoil plus cavity, onto the upper half of the plane exterior to the unit circle. The complex acceleration potential is used, and its real part is specified on the real axis, representing the cavity boundary, while its imaginary part is specified on the unit semicircle, representing the wetted surface of the airfoil and spoiler. Solutions are found for both the steady-state lift and the transient lift after spoiler actuation for airfoils of arbitrary camber, thickness and incidence, with and without a simple flap, and with spoilers of arbitrary position, height and angle. The empirical cavity pressure is arbitrary for the steady-state solution, but is assumed to have the free-stream value for the transient solutions. Comparisons are made with the results of wind-tunnel experiments, and, for the steady-state solutions, with predictions of an earlier theory. The agreement of the present theoretical predictions with the experimental results is generally good, and is in most cases somewhat better than that of the earlier theory.

1. Introduction

Upper surface spoilers on lifting airfoils are in general use as devices to reduce lift and increase drag, and although there is an increased interest in their additional use for roll control of STOL aircraft, there has been relatively little general information, either experimental or theoretical, available on their performance characteristics, particularly the transient characteristics.

The problem of developing a satisfactory theory is made more difficult by the present general inability to predict wake properties of separated flows. As a result, any theoretical model for an airfoil with spoiler will include some empiricism. However, the separation points are fixed at the spoiler tip and airfoil trailing edge, and the separating shear layers are thin and well-defined close to the airfoil, so that an irrotational free-streamline model of the flow outside the wake should be capable of producing accurate results, except for any boundary-layer-separation bubble caused by the positive pressure gradient in front of the spoiler. Some empirical data on the flow conditions at the edges of the wake is needed to complete such an irrotational model.

In an earlier linearized two-dimensional theory, Woods (1953) assumed that the pressure *change* caused by the spoiler is constant between the spoiler and the trailing edge of the airfoil. This constant, and an additional symmetrical boundary pressure distribution representing the effect of the infinite wake downstream of the airfoil's trailing edge, are supposed to be given empirically. He developed a free-streamline model using conformal transformations involving the complex potential and velocity, and solved for the loading on the airfoil as a function of geometric parameters of the spoiler. Subsequently, Barnes (1965) devised an empirical modification to Woods's theory for normal spoilers, accounting for the effect of the airfoil boundary layer on the effective height of a spoiler, and providing an empirical formula for the incremental spoiler base pressure.

Other models of partially separated flows over foil sections have been developed for cavitating hydrofoils, and for these also two-dimensional irrotational flow theory is suitable. The necessary empiricism is usually introduced by specifying both a constant cavity pressure and the nature of the downstream closure of the finite cavity. Parkin (1959) has applied the method of complex acceleration potential introduced by Biot (1942) to a linearized problem of this class, that of the loading on fully cavitating hydrofoils in non-steady motion, and Fabula (1962) has applied the same method to the case of a hydrofoil in steady motion with the cavity starting at an arbitrary point on the upper surface. Song (1965) has applied the method to a supercavitating flat-plate hydrofoil with an oscillating flap.

The above theoretical models are all linearized, and consequently might be expected to predict forces and moments successfully, but not pressure distributions. For these, a thick-airfoil theory is needed, and Jandali & Parkinson (1970) have developed one for Joukowsky airfoils with normal spoilers, using a sequence of conformal transformations and a modification of the wake source model of Parkinson & Jandali (1970). This theory has been extended to apply to solid airfoils of arbitrary profile with normal spoilers by Jandali (1970), using an adaptation of the method of Theodorsen (1931), and to airfoils with inclined spoilers and slotted flaps by Brown (1971), using a combination of the surface source distribution method of Hess & Smith (1966) and the above wake source model.

The present work is intended to provide an improved steady two-dimensional thin-airfoil theory for the prediction of forces and moments on solid airfoils with spoilers, and to extend the theory to predict the transient loading following spoiler actuation. The constant-cavity-pressure assumption used in the hydrofoil models is more realistic for the base pressure of the airfoil with spoiler than is Woods's assumption of a constant incremental pressure, since experiments demonstrate that the actual pressure, and not its increment caused by the spoiler, is constant behind the spoiler for a given configuration (see, for example, Jandali & Parkinson 1970, figures 5–10). Accordingly, the method of Parkin (1959), with a finite constant-pressure cavity analysed in terms of the complex acceleration potential, is adapted to the present problem.

Apart from the different method of treating the wake, and a different mathematical model, the present steady theory differs from that of Woods (1953) in its

inclusion of the effect of airfoil thickness, which Woods neglects. In conventional thin-airfoil theory without flow separation, there is no effect of thickness on the lift and moment. However, the presence of the spoiler removes the upper surface of the basic airfoil behind the spoiler from the effective flow field, so the effective thickness envelope of the airfoil with spoiler becomes asymmetric, and now has an effect on the lift and moment, in addition to the direct effect of the spoiler and of the airfoil incidence and camber.

In the following section, the theory is developed for a thin solid airfoil of small but arbitrary camber, thickness and incidence with or without a simple flap, and with a small spoiler of arbitrary height, location and inclination. For the steady theory, the spoiler base pressure is a constant, determined from experiment. For the transient theory, the base pressure is taken to have the free-stream value.

2. General theory

2.1. *Acceleration potential*

Biot (1942) showed that a two-dimensional incompressible irrotational flow past a thin airfoil could be conveniently analysed in terms of an acceleration potential, which exists because the fluid acceleration vector is the gradient of a scalar function, the negative pressure–density ratio. Parkin (1959) presented a comprehensive treatment of the acceleration potential and its application to thin cavitating hydrofoils. For steady flow, the cavity surface velocity magnitude is constant and is used by Parkin as the fundamental reference velocity. In the usual linearized airfoil problem without cavitation, the undisturbed velocity at infinity U is the only characteristic velocity and it is convenient to retain it here as the reference velocity. Thus at any point (x, y) in the non-steady flow around the airfoil the velocity vector $\mathbf{q}$ can be expressed in terms of dimensionless components (u, v) as

$$\mathbf{q}(x, y, t) = U\{(1+u), v\}.$$

The cavity pressure p_c is constant and can be related to the reference pressure at infinity p_∞ by the cavitation number K. The pressure coefficient C_p has its customary definition and the base pressure coefficient C_{pb} is related to K by

$$K = \frac{p_\infty - p_c}{\frac{1}{2}\rho U^2} = -C_{pb}.$$

The acceleration potential ϕ is easily shown to be a harmonic function, so a conjugate function ψ can be introduced, and a complex acceleration potential defined by the analytic function

$$F(z, t) = \phi(x, y, t) + i\psi(x, y, t), \tag{2.1}$$

where $z = x + iy$.

Using the Euler and Cauchy–Riemann equations the x and y components of the perturbation velocity can be related to ϕ and ψ by the linear first-order differential equations

$$\frac{\partial u}{\partial t} + U\frac{\partial u}{\partial x} = U\frac{\partial \phi}{\partial x}$$

and

$$\frac{\partial v}{\partial t} + U\frac{\partial v}{\partial x} = -U\frac{\partial \psi}{\partial x},$$

where ϕ and ψ, but not x, y or t, have been defined in dimensionless form.

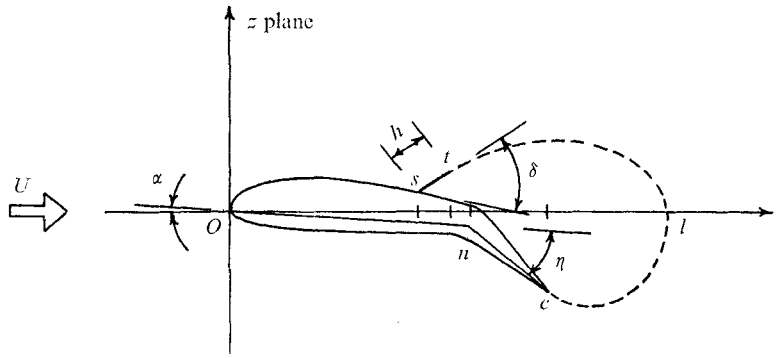

FIGURE 1. Airfoil in physical plane.

For the special case of steady flow, these equations reduce to

$$u = \phi + \tfrac{1}{2}K, \quad v = -\psi, \tag{2.2}$$

where the constants of integration have been determined by the conditions at infinity, and by choosing the constant value of ϕ on the cavity boundary to be zero. The usual linearized pressure coefficient can then be determined as

$$C_p = -2\phi - K. \tag{2.3}$$

Using the Blasius equation and integrating along a contour enclosing the body cavity system, the lift coefficient can be expressed in terms of the first-order dimensionless perturbation velocities. Introduction of (2.1) and (2.2) gives the lift coefficient as

$$C_D - iC_L = \frac{2i}{c}\oint F(z)\,dz, \tag{2.4}$$

where c is the airfoil chord length.

2.2. *Transformations*

An airfoil of chord c, spoiler height h and flap chord c_η is immersed in a two-dimensional, incompressible, irrotational flow uniform at infinity. The airfoil leading edge is positioned at the origin of the z plane as shown in figure 1, and a fully developed closed cavity of length l extends from separation points t and c, the spoiler tip and the airfoil trailing edge respectively. The upstream part sOc of the body contour C is mapped conformally from the upper half of the unit circle γ, in the ζ plane, by the analytic function

$$z = f(\zeta) = \frac{la^{-2}[\frac{1}{4}(b+1)(\zeta+\zeta^{-1}) - \frac{1}{2}(1-b)]^2}{1 + a^{-2}[\frac{1}{4}(b+1)(\zeta+\zeta^{-1}) - \frac{1}{2}(1-b)]^2},$$
$$a = [(l-c)/c]^{\frac{1}{2}}, \quad b = a[t/(l-t)]^{\frac{1}{2}}. \tag{2.5}$$

The linearized physical, intermediate and final transform planes are shown in figure 2. In the ζ plane, the cavity extends along the real axis $\zeta > 1$ and $\zeta < -1$, and $z = -\infty$, where the boundary conditions at infinity are to be applied, maps to the point

$$\zeta_i = \frac{2}{1+b}\left[ia + \frac{1-b}{2}\right] + \left[\left(\frac{2}{1+b}\right)^2\left\{ia + \frac{1-b}{2}\right\}^2 - 1\right]^{\frac{1}{2}}. \tag{2.6}$$

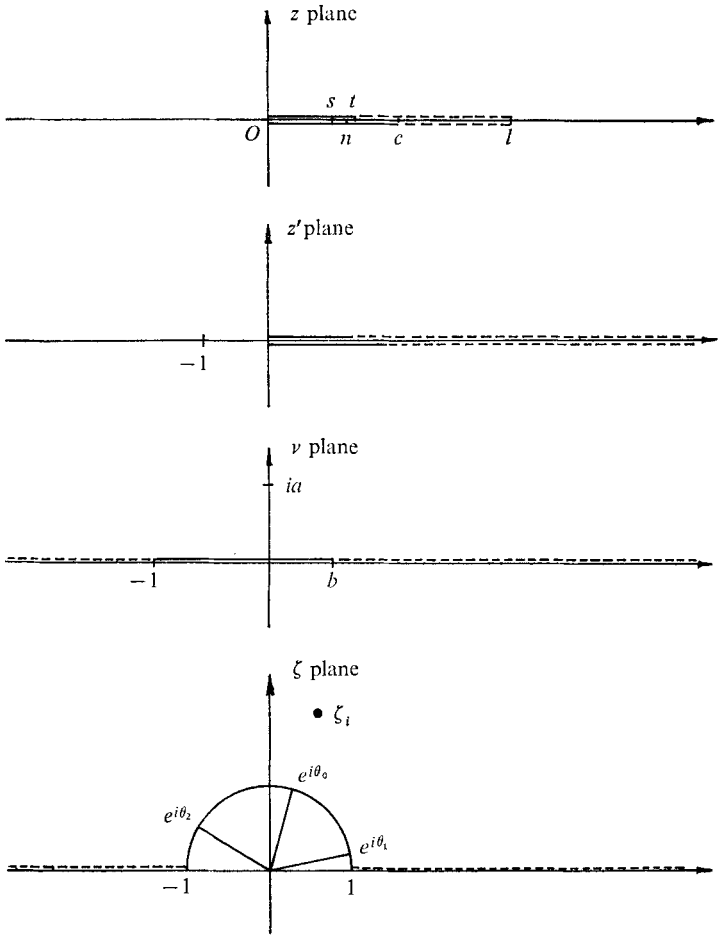

FIGURE 2. Complex transform planes.

The angular locations of points O, s and n in the ζ plane can be determined from (2.4) as

$$\theta_0 = \cos^{-1}[(1-b)/(1+b)],$$

$$\theta_1 = \cos^{-1}\left[\frac{2}{1+b}\left\{a\left(\frac{s}{l-s}\right)^{\frac{1}{2}}+\frac{1-b}{2}\right\}\right]$$

and

$$\theta_2 = \cos^{-1}\left[\frac{2}{1+b}\left\{\frac{1-b}{2}-a\left(\frac{c-c_\eta}{l-c+c_\eta}\right)^{\frac{1}{2}}\right\}\right],$$

where the inverse cosines are taken between zero and π. The complex acceleration potentials in the transform planes are invariant at corresponding points and the accelerations differ only by the derivative of the mapping functions, and thus

$$\frac{dF}{d\zeta} = \frac{dF}{dz}\frac{dz}{d\zeta}.$$

3. Steady theory

3.1. *Boundary conditions*

The steady-state boundary conditions are as follows.

(i) $\phi = \mathrm{Re}\, F = 0$ on the cavity, $l \geqslant x \geqslant t$, $y = 0^+$ and $l \geqslant x \geqslant c$, $y = 0^-$.

(ii) Kutta conditions ϕ continuous at the spoiler tip $x = t$, $y = 0^+$ and at the airfoil trailing edge $x = c$, $y = 0^-$.

(iii) Airfoil surface normal boundary condition

$$v = -\psi = dy/dx,$$

where the airfoil surface is denoted by $(x, y(x))$.

(iv) The boundary condition $F = -\frac{1}{2}K$ at infinity.

(v) The body and cavity system must be equivalent to a single closed body. The condition of zero drag on this equivalent body is used in (2.4), and this leads to the condition

$$\mathrm{Im} \oint_{\Gamma} F(z)\, dz = 0, \tag{3.1}$$

where the contour of integration again encloses the body and cavity system.

3.2. *Flow model*

A common thin-airfoil-theory approach is followed with the determination of a set of complex functions in the ζ plane that satisfy the above boundary conditions. Incidence, camber, thickness, spoiler and flap solutions can be determined independently and then superposed.

Incidence case. Consider the complex functions

$$F_{in}(\zeta) = iC_0 \left[\frac{1}{\zeta e^{i\theta_0} - 1} + \frac{1}{\zeta e^{-i\theta_0} - 1} \right] + iB_0 \left(\zeta - \frac{1}{\zeta} \right) + iD_0, \tag{3.2}$$

where B_0, C_0 and D_0 are real constants. The first term provides the usual thin-airfoil singularity at the point corresponding to the airfoil leading edge. The conjugate term is necessary to satisfy the boundary condition and maintain the unit circle and real axis as a streamline. The cavity termination must be a singular point to account for the branching of the free streamlines. In the ζ plane this point is located at infinity on the real axis. A simple pole at the origin, the inverse point for the cavity closure in the unit circle, is added to the second term to satisfy the streamline boundary conditions. The third term, a complex constant, also does not violate these conditions and is an acceptable function. Boundary conditions (iii)–(v) are still to be satisfied.

Camber case. Consider the function

$$F_c(\zeta) = -i \sum_{1}^{\infty} \frac{M_n}{\zeta^n}, \tag{3.3}$$

where the M_n are real constants. The free-streamline and Kutta conditions are clearly satisfied. Boundary condition (iii) can be used in conjunction with the known Fourier series for dy/dx for this case, $(dy/dx)_c$, to give the unknown M_n as

$$M_n = \frac{2}{\pi} \int_0^{\pi} \left(\frac{dy}{dx} \right) \cos n\theta\, d\theta. \tag{3.4}$$

With a combination of incidence and camber

$$dy/dx = -\operatorname{Im} F = C_0 - D_0 + \sum_1^\infty M_n \cos n\theta = -\alpha + (dy/dx)_c.$$

It follows that $$D_0 = \alpha - \tfrac{1}{2}M_0 + C_0,$$

where $$M_0 = \frac{2}{\pi}\int_0^\pi \left(\frac{dy}{dx}\right)_c d\theta.$$

The constants B_0 and C_0 are still to be determined.

Thickness case. For the thickness solution consider the complex function

$$F_t(\zeta) = \frac{i\zeta}{(\zeta - e^{i\theta_0})(\zeta - e^{-i\theta_0})} \sum_0^\infty \frac{N_n}{\zeta^n}, \tag{3.5}$$

where the N_n are real constants. This function satisfies the free-streamline and Kutta conditions and the unknown N_n can be solved for, as in the camber solution, through application of boundary condition (iii). For the thickness case $dy/dx \equiv (dy/dx)_t$ as a function of θ is not continuous as in the camber solution, but has a discontinuity at the point corresponding to the airfoil leading edge. Determination of the unknown N_n does however reduce to the solution of a Fourier series. The coefficients N_n are given by

$$N_n = \frac{4}{\pi}\int_0^\pi \left(\frac{dy}{dx}\right)_t (\cos\theta_0 - \cos\theta)\cos n\theta \, d\theta, \quad n \geqslant 1,$$

and $$N_0 = \frac{2}{\pi}\int_0^\pi \left(\frac{dy}{dx}\right)_t (\cos\theta_0 - \cos\theta)\, d\theta.$$

It was found necessary to use a complex thickness function with a singularity at the point corresponding to the airfoil leading edge. In attempting to use a function similar to that of the camber case, it was found that the Fourier coefficients would not converge.

Spoiler case. In the spoiler case, there is a step change in v passing along the body contour across the point corresponding to the spoiler base. It is also required that v be constant over the appropriate portions of the unit circle. Parkin (1959) demonstrated that a combination of logarithmic terms will satisfy such constraints. It is convenient to combine such a function with one of the same type as the first term from the incidence case to give the spoiler function

$$F_s(\zeta) = \frac{\sin\delta}{\pi}\left[\frac{i\theta_1}{\zeta e^{i\theta_0} - 1} + \frac{i\theta_1}{\zeta e^{-i\theta_0} - 1} + \ln\left\{\frac{\zeta - e^{i\theta_1}}{\zeta - e^{-i\theta_1}}\right\}\right]. \tag{3.6}$$

Applying boundary condition (iii) to (3.6) gives

$$v = \begin{cases} 0 & \text{on the foil} \quad \pi > \theta > \theta_1, \\ \sin\delta & \text{on the spoiler} \quad \theta_1 > \theta > 0. \end{cases}$$

Although its use is inconsistent with the assumptions of linearized theory, $\sin\delta$ replaces δ in the above boundary condition so that spoiler angles up to 90°

can be considered realistically. Both Woods (1953) and Barnes (1965) have had some success with normal spoilers using linearized theories. It was demonstrated in the incidence case that the first term of (3.6) satisfies the first two boundary conditions. On the cavity where $|\zeta| \geqslant 1$ and ζ is real, the logarithm term is purely imaginary and hence satisfies both the streamline and Kutta conditions.

Flap case. This case is identical to the spoiler case except that the flap is restricted to small angles. The complex flap function is

$$F_f(\zeta) = \frac{\eta}{\pi}\left[\frac{i(\theta_2-\pi)}{\zeta e^{i\theta_0}-1} + \frac{i(\theta_2-\pi)}{\zeta e^{-i\theta_0}-1} + \ln\left\{\frac{\zeta - e^{i\theta_2}}{\zeta - e^{-i\theta_2}}\right\}\right]. \tag{3.7}$$

The perturbation velocity v on the surface for this case is determined from boundary condition (iii) to be

$$v = \begin{cases} 0 & \text{on the foil} \quad \theta_2 > \theta > 0, \\ -\eta & \text{on the flap} \quad \pi > \theta > \theta_2. \end{cases}$$

It has been demonstrated in the spoiler case that the functions (3.7) satisfy the first two boundary conditions.

The constants B_0 and C_0 remain unknown, and will be determined by application of boundary condition (iv) to the real and imaginary parts of the complex functions developed in this subsection. Boundary condition (v) enables a relationship between the cavity number K and cavity length l to be established.

3.3. *Method of solution*

Boundary condition (iv), the condition at infinity, can be expressed as

$$F_{in}(\zeta_i) + F_c(\zeta_i) + F_t(\zeta_i) + F_s(\zeta_i) + F_f(\zeta_i) = -\tfrac{1}{2}K,$$

where ζ_i, the point at infinity, was given by (2.6). The unknown constants B_0 and C_0 are contained in $F_{in}(\zeta_i)$. The real and imaginary parts of this equation give two simultaneous equations in C_0 and B_0. The values of these constants are

$$B_0 = \frac{\operatorname{Re}\lambda_1[\operatorname{Im}E - (\alpha - \frac{1}{2}M_0)] - \operatorname{Im}\lambda_1 \operatorname{Re}E + \frac{1}{2}K \operatorname{Im}\lambda_1}{\operatorname{Re}\lambda_1 \operatorname{Im}\lambda_2 - \operatorname{Im}\lambda_1 \operatorname{Re}\lambda_2}$$

and

$$C_0 = (\operatorname{Re}E - B_0 \operatorname{Re}\lambda_2 - \tfrac{1}{2}K)/\operatorname{Re}\lambda_1,$$

where

$$\lambda_1 = i\left[\frac{1}{\zeta_i e^{i\theta_0}-1} + \frac{1}{\zeta_i e^{-i\theta_0}-1} + 1\right], \quad \lambda_2 = i\left(\zeta_i - \frac{1}{\zeta_i}\right)$$

and

$$E = -F_c(\zeta_i) - F_t(\zeta_i) - F_s(\zeta_i) - F_f(\zeta_i).$$

All the function constants have been determined. Still unknown are K and l. There is not currently a theory that will correctly predict the base pressure for separated flows and at least this parameter will be an empirical input. Since l can be related to K through boundary condition (v), no further input is required. Choosing a contour such that $|z| \gg l$, ζ can be expressed as a Laurent expansion. The closure condition becomes

$$\operatorname{Re}\{\text{coefficient of } z^{-1}\} = 0.$$

Solving this equation gives K in terms of l as

$$K = 2\,\mathrm{Re}\left\{ la_1\left(i\left(1+\frac{1}{a_0^2}\right)\left[\frac{\mathrm{Re}\,\lambda_1[\mathrm{Im}\,E-(\alpha-\frac{1}{2}M_0)]-\mathrm{Im}\,\lambda_1\,\mathrm{Re}\,E}{\mathrm{Re}\,\lambda_1\,\mathrm{Im}\,\lambda_2-\mathrm{Im}\,\lambda_1\,\mathrm{Re}\,\lambda_2}\right]\right.\right.$$
$$-i\left[\frac{e^{i\theta_0}}{(a_0e^{i\theta_0}-1)^2}+\frac{e^{-i\theta_0}}{(a_0e^{-i\theta_0}-1)^2}\right]\left[\frac{\mathrm{Re}\,\lambda_2[\mathrm{Im}\,E-(\alpha-\frac{1}{2}M_0)]-\mathrm{Im}\,\lambda_2\,\mathrm{Re}\,E}{\mathrm{Re}\,\lambda_2\,\mathrm{Im}\,\lambda_1-\mathrm{Im}\,\lambda_2\,\mathrm{Re}\,\lambda_1}\right.$$
$$\left.+\frac{\theta_1\sin\delta}{\pi}+\frac{\theta_2-\pi}{\pi}\eta\right]$$
$$+\frac{\sin\delta}{\pi}\left[\frac{1}{a_0-e^{i\theta_1}}-\frac{1}{a_0-e^{-i\theta_1}}\right]+\frac{\eta}{\pi}\left[\frac{1}{a_0-e^{i\theta_2}}-\frac{1}{a_0-e^{-i\theta_2}}\right]$$
$$\left.+i\sum_1^\infty\frac{nM_n}{a_0^{n+1}}+i\sum_0^\infty N_n\frac{\left[\frac{1-n}{a_0}-\frac{e^{i\theta_0}}{a_0e^{i\theta_0}-1}-\frac{e^{-i\theta_0}}{a_0e^{-i\theta_0}-1}\right]}{a_0^{n-1}(a_0e^{i\theta_0}-1)(a_0e^{-i\theta_0}-1)}\right)\Bigg\}\Bigg/$$
$$\mathrm{Re}\left\{ la_1\left(i\frac{\mathrm{Im}\,\lambda_2}{\mathrm{Re}\,\lambda_2\,\mathrm{Im}\,\lambda_1-\mathrm{Im}\,\lambda_2\,\mathrm{Re}\,\lambda_1}\left[\frac{e^{i\theta_0}}{(a_0e^{i\theta_0}-1)^2}+\frac{e^{-i\theta_0}}{(a_0e^{-i\theta_0}-1)^2}\right]\right.\right.$$
$$\left.\left.-i\frac{\mathrm{Im}\,\lambda_1}{\mathrm{Re}\,\lambda_1\,\mathrm{Im}\,\lambda_2-\mathrm{Im}\,\lambda_1\,\mathrm{Re}\,\lambda_2}\left(1+\frac{1}{a_0^2}\right)\right)\right\}, \quad (3.8)$$

where
$$a_0=\frac{1-b}{1+b}+\frac{2ia}{1+b}+\left[\left\{\frac{1-b}{1+b}+\frac{2ia}{1+b}\right\}^2-1\right]^{\frac{1}{2}}$$

and
$$a_1=\frac{ia}{1+b}\left[1+\frac{\frac{1-b}{1+b}+\frac{2ia}{1+b}}{\left[\left\{\frac{1-b}{1+b}+\frac{2ia}{1+b}\right\}^2-1\right]^{\frac{1}{2}}}\right].$$

An iterative or graphical technique is necessary to solve (3.8) because θ_0, θ_1 and θ_2 are complex functions of l.

This completes the problem formulation for the steady theory and it remains to determine the pressure and lift coefficients. Using (3.8), and collecting the values of the acceleration potentials (which are the real parts of (3.2), (3.3), (3.5), (3.6) and (3.7)), the pressure coefficient, as a function of angular position on the unit circle in the ζ plane, can be written as

$$C_p=-2\left[C_0+\frac{\eta(\theta_2-\pi)}{\pi}+\frac{\theta_1\sin\delta}{\pi}\right]\frac{\sin\theta}{\cos\theta_0-\cos\theta}+4B_0\sin\theta$$
$$-\frac{2\sin\delta}{\pi}\ln\left\{\frac{\sin\frac{1}{2}|\theta-\theta_1|}{\sin\frac{1}{2}(\theta+\theta_1)}\right\}-\frac{2\eta}{\pi}\ln\left\{\frac{\sin\frac{1}{2}|\theta-\theta_2|}{\sin\frac{1}{2}(\theta+\theta_2)}\right\}$$
$$+2\sum_1^\infty M_n\sin n\theta+\frac{\sum_1^\infty N_n\sin n\theta}{\cos\theta_0-\cos\theta}-K,$$

where points on the airfoil can be related through the transformation (2.5) to points on the unit circle by

$$x=\frac{la^{-2}[\frac{1}{2}(b+1)\cos\theta-\frac{1}{2}(1-b)]^2}{1+a^{-2}[\frac{1}{2}(b+1)\cos\theta-\frac{1}{2}(1-b)]^2}.$$

The lift coefficient can be determined by the use of (2.4) and the Laurent expansion determined from application of boundary condition (v). The lift and drag coefficients are given by

$$\left.\begin{aligned} C_L &= \frac{4\pi}{c}\,\mathrm{Im}\left\{\text{coefficient of } \frac{1}{z}\right\} \\ \text{and} \qquad C_D &= -\frac{4\pi}{c}\,\mathrm{Re}\left\{\text{coefficient of } \frac{1}{z}\right\}. \end{aligned}\right\} \tag{3.9}$$

The real part of the coefficient of z^{-1} was shown to be zero in the consideration of the closure condition, so the overall drag coefficient is zero as expected in potential flow theory. The drag on the airfoil is balanced by the force on the singularity at the cavity termination and this point only need be considered in (3.9) to determine the airfoil drag. The drag predicted is unrealistically high. This result is probably due to the theory being unable to model the separation bubble evident in real flow in front of the spoiler. The drag theory therefore will not be pursued further. The lift coefficient becomes

$$\begin{aligned} C_L = \frac{4\pi}{c}\,\mathrm{Im}\Bigg\{ & iB_0 l a_1\left(1+\frac{1}{a_0^2}\right) - i\left[C_0+\frac{\theta_1\sin\delta}{\pi}+\frac{(\theta_2-\pi)\eta}{\pi}\right] \\ & \times l a_1\left[\frac{e^{i\theta_0}}{(a_0 e^{i\theta_0}-1)^2}+\frac{e^{-i\theta_0}}{(a_0 e^{-i\theta_0}-1)^2}\right]+\frac{\sin\delta}{\pi}\,l a_1\left[\frac{1}{a_0-e^{i\theta_1}}-\frac{1}{a_0-e^{-i\theta_1}}\right] \\ & +\frac{\eta}{\pi}\,l a_1\left[\frac{1}{a_0-e^{i\theta_2}}-\frac{1}{a_0-e^{-i\theta_2}}\right]+il a_1\sum_1^\infty \frac{nM_n}{a_0^{n+1}} \\ & +il a_1\sum_0^\infty N_n\,\frac{\left[\dfrac{1-n}{a_0}-\dfrac{e^{i\theta_0}}{a_0 e^{i\theta_0}-1}-\dfrac{e^{-i\theta_0}}{a_0 e^{-i\theta_0}-1}\right]}{a_0^{n-1}(a_0 e^{i\theta_0}-1)(a_0 e^{-i\theta_0}-1)}\Bigg\}. \end{aligned}$$

The Blasius equation for the pitching moment could be applied to determine the pitching-moment coefficient of the airfoil. This has not yet been attempted.

4. Non-steady theory

The non-steady problem considered in this paper is the case of spoiler actuation on a fixed airfoil in initially steady flow. Non-steady airfoil motions with fixed spoiler angles have not been considered. Such cases are a much simpler application of this theory and have many features in common with existing results given by Parkin (1959). The spoiler actuation theory is developed for the case of zero cavitation number. In the present analysis, it is not possible to allow the cavitation number to be a function of time since this would make the cavity length, and hence the transformations, a function of time. Modification of the current theory would be necessary to effect a solution in such a situation. The only relatively simple approaches would appear to be either to assume that as soon as the spoiler starts to move the cavity number takes its final steady-state value, or to assume that the cavity number is at all times zero. The first assumption has limitations and the second, although not physically realized, does have merit. The average pressure on the rear part of the upper surface of an airfoil in most configurations

is very close to zero. Hence during the initial part of the spoiler actuation, the cavitation number is close to zero. Also the zero-cavitation-number solution is simpler mathematically and its complete linearity permits easy comparisons with solutions of existing non-steady thin-airfoil problems such as change of angle of attack. At zero cavitation number the cavity pressure is equal to the undisturbed free-stream static pressure and the cavity extends to infinity. The foil is positioned as shown in figure 1 for the steady flow solution, with $l = \infty$.

Linear airfoil techniques are once again employed, and solutions are to be obtained for the unit step spoiler actuation and the finite time spoiler actuation. In the problem of a unit step change of angle of attack in existing thin-airfoil theory (see Bisplinghoff, Ashley & Halfman 1955), an intermediate solution to the harmonically plunging airfoil problem is required. An analogous approach is used in this paper, although the spoiler moves relative to a fixed airfoil. The boundary condition on the spoiler is a step in the v component of velocity given by $v = \sin\delta$. Such a step change in velocity can be achieved by solving for the case of a sinusoidal velocity of circular frequency ω, $v = v_0 e^{j\omega t}$, over this region and then integrating over all frequencies. This velocity is considered to be a disturbance to the existing steady-state solution for some spoiler angle. This problem will henceforth be referred to as 'blowing' theory.

4.1. *Blowing theory*

Only the flat plate of zero incidence need be considered. This problem is equivalent to the spoiler case from the steady solution and the remaining steady-state solutions of incidence, camber, thickness and flap for $K = 0$ are fully additive to this non-steady solution.

4.2. *Boundary conditions and transformations*

Boundary conditions (i), (ii) and (iv) for this non-steady blowing problem remain the same as for the steady-state solution. The remaining boundary conditions are

$$\text{(iii)} \quad v = \begin{cases} 0 & \text{on the foil} \quad 0 \leqslant x \leqslant s,\ y = 0^+ \quad \text{and} \quad 0 \leqslant x \leqslant c,\ y = 0^-, \\ v_0 e^{j\omega t} & \text{on the spoiler} \quad s \leqslant x \leqslant t,\ y = 0^+; \end{cases}$$

$$\text{(v)} \quad \operatorname{Im}\frac{dF}{dz} = \begin{cases} 0 & \text{on the foil} \quad 0 \leqslant x \leqslant s,\ y = 0^+ \quad \text{and} \quad 0 \leqslant x \leqslant c,\ y = 0^-, \\ -j\mu v_0 e^{j\omega t} & \text{on the spoiler} \quad s \leqslant x \leqslant t,\ y = 0^+. \end{cases}$$

The frequency parameter μ is given by $\mu = \omega/U$. The physical plane for this problem is the z plane of figure 2 with $l = \infty$, and the basic transform plane remains essentially the same as the ζ plane. The analytic transformation function is

$$\left.\begin{aligned} z = f(\zeta) &= \frac{1}{a'^2}\left[\frac{b'+1}{4}\left(\zeta+\frac{1}{\zeta}\right) - \frac{1-b'}{2}\right]^2, \\ a' &= [1/c]^{\frac{1}{2}}, \quad b' = a' t^{\frac{1}{2}}. \end{aligned}\right\} \tag{4.1}$$

Points on the airfoil contour C in the z plane are related to the corresponding points on the unit circle contour γ by

$$\frac{x}{c} = \left(\frac{b'+1}{2}\right)^2 [\cos\theta - \cos\theta_0]^2. \tag{4.2}$$

4.3. *Method of solution*

Integration of boundary condition (v) gives

$$\psi = \begin{cases} C_2 e^{j\omega t} & \text{on the foil,} \\ -j\mu v_0 e^{j\omega t}\left[\left(\frac{b'+1}{2}\right)^2 \times \tfrac{1}{2}\cos 2\theta - \left(\frac{1-b'^2}{2}\right)\cos\theta\right] + C_1 e^{j\omega t} & \text{on the spoiler,} \end{cases} \tag{4.3}$$

where the 'constants' of integration are assumed to be harmonic functions of t. The solution to this problem closely follows the techniques of the steady-state problem. Complex functions must be determined to satisfy the boundary conditions. The constant terms of (4.3) can be satisfied by functions presented in the steady-state spoiler case, and the remaining term is of the camber type that can be represented by a Fourier series complex function. The non-steady complex function can then be written in terms of the unknowns C_1 and C_2 as

$$F_n(\zeta) = -j\mu v_0 e^{j\omega t} i \sum_1^\infty \frac{J_n}{\zeta^n} - \frac{C_1 e^{j\omega t}}{\pi}\left[\frac{i\theta_1}{\zeta e^{i\theta_0}-1} + \frac{i\theta_1}{\zeta e^{-i\theta_0}-1} + \ln\left\{\frac{\zeta - e^{i\theta_1}}{\zeta - e^{-i\theta_1}}\right\}\right]$$
$$+ \frac{C_2 e^{j\omega t}}{\pi}\left[\frac{i(\theta_1-\pi)}{\zeta e^{i\theta_0}-1} + \frac{i(\theta_1-\pi)}{\zeta e^{-i\theta_0}-1} + \ln\left\{\frac{\zeta - e^{i\theta_1}}{\zeta - e^{-i\theta_1}}\right\}\right], \tag{4.4}$$

where

$$J_n = \frac{2}{\pi}\int_0^\pi f(\theta)\cos n\theta\, d\theta \tag{4.5}$$

and

$$f(\theta) = \begin{cases} \left(\frac{b'+1}{2}\right)^2 \times \tfrac{1}{2}\cos 2\theta - \left(\frac{1-b'^2}{2}\right)\cos\theta & (\theta_1 \geqslant \theta \geqslant 0), \\ 0 & (\pi \geqslant \theta \geqslant \theta_1). \end{cases}$$

In (4.5) the constant Fourier coefficient has been absorbed in C_1. The complex functions are of the steady-state type and clearly satisfy boundary conditions (i) and (ii). Boundary condition (v) was used to determine the non-steady complex functions and is inherently satisfied. Consideration of the mapping function (4.1) and of (4.4) shows that F_n approaches zero as $|z|$ approaches infinity. Boundary condition (iv) is therefore satisfied. Boundary condition (iii) can now be used to determine the unknown constants C_1 and C_2. To first order in the perturbations, the v component of Euler's equations of motion may be written as

$$\frac{dV_0}{dx} + j\mu V_0 = -\frac{\partial \psi_0}{\partial x}, \tag{4.6}$$

where the non-steady complex function has been expressed as

$$F_n(\zeta) = [\phi_0(\zeta) + i\psi_0(\zeta)]\, e^{j\omega t}$$

and

$$v = V_0 e^{j\omega t}.$$

Since V_0, the velocity amplitude of a given point in the flow field about the x axis, must vanish at infinity, the integral of (4.6) becomes

$$V_0 = -e^{-j\mu x}\int_{-\infty}^{x} \frac{\partial \psi_0}{\partial \xi} e^{j\mu\xi}\, d\xi,$$

where x refers to any point on the airfoil or spoiler and ξ is a streamwise variable of integration. At points on the airfoil $V_0 = 0$ and at points on the spoiler $V_0 = v_0$. Consideration of two such points results in two simultaneous equations in the two unknowns C_1 and C_2. The solution of these equations is

$$C_1 = -v_0 \frac{\left\{\left[j\mu\int_0^\infty e^{-j\mu\xi'} T_3 d\xi' - \pi\right] \times \left[j\mu\left\{\frac{1}{2}\left(\frac{b'+1}{2}\right)^2 \cos 2\theta_1 - \left(\frac{1-b'^2}{2}\right)\cos\theta_1\right\} - 1\right] - \mu^2\pi\int_0^\infty e^{-j\mu\xi'} T_1 d\xi'\right\}}{\pi\left\{1 + j\mu\int_0^\infty e^{-j\mu\xi'} T_4 d\xi'\right\}}$$

and

$$C_2 = \frac{v_0\pi\mu^2\int_0^\infty e^{-j\mu\xi'} T_1 d\xi' - j\mu C_1\int_0^\infty e^{-j\mu\xi'} T_2 d\xi'}{\pi - j\mu\int_0^\infty e^{-j\mu\xi'} T_3 d\xi'},$$

where

$$T_1 = \mathrm{Re}\sum_1^\infty \frac{J_n}{\left[\cos\theta_0 + \frac{2i}{1+b'}\xi'^{\frac{1}{2}} + \left\{\left[\cos\theta_0 + \frac{2i}{1+b'}\xi'^{\frac{1}{2}}\right]^2 - 1\right\}^{\frac{1}{2}}\right]^n},$$

$$T_2 = \mathrm{Re}\left\{\theta_1\left[\frac{\left\{\left[\cos\theta_0 + \frac{2i}{1+b'}\xi'^{\frac{1}{2}}\right]^2 - 1\right\}^{\frac{1}{2}}}{\frac{2i}{1+b'}\xi'^{\frac{1}{2}}} - 1\right] + \arg\left\{\frac{\cos\theta_0 + \frac{2i}{1+b'}\xi'^{\frac{1}{2}} + \left\{\left[\cos\theta_0 + \frac{2i}{1+b'}\xi'^{\frac{1}{2}}\right]^2 - 1\right\}^{\frac{1}{2}} - e^{i\theta_1}}{\cos\theta_0 + \frac{2i}{1+b'}\xi'^{\frac{1}{2}} + \left\{\left[\cos\theta_0 + \frac{2i}{1+b'}\xi'^{\frac{1}{2}}\right]^2 - 1\right\}^{\frac{1}{2}} - e^{-i\theta_1}}\right\}\right\},$$

$$T_3 = \mathrm{Re}\left\{(\theta_1 - \pi)\left[\frac{\left\{\left[\cos\theta_0 + \frac{2i}{1+b'}\xi'^{\frac{1}{2}}\right]^2 - 1\right\}^{\frac{1}{2}}}{\frac{2i}{1+b'}\xi'^{\frac{1}{2}}} - 1\right] + \arg\left\{\frac{\cos\theta_0 + \frac{2i}{1+b'}\xi'^{\frac{1}{2}} + \left\{\left[\cos\theta_0 + \frac{2i}{1+b'}\xi'^{\frac{1}{2}}\right]^2 - 1\right\}^{\frac{1}{2}} - e^{i\theta_1}}{\cos\theta_0 + \frac{2i}{1+b'}\xi'^{\frac{1}{2}} + \left\{\left[\cos\theta_0 + \frac{2i}{1+b'}\xi'^{\frac{1}{2}}\right]^2 - 1\right\}^{\frac{1}{2}} - e^{-i\theta_1}}\right\}\right\}$$

and

$$T_4 = \mathrm{Re}\left\{\frac{\left\{\left[\cos\theta_0 + \frac{2i}{1+b'}\xi'^{\frac{1}{2}}\right]^2 - 1\right\}^{\frac{1}{2}}}{\left[\frac{2i}{1+b'}\right]\xi'^{\frac{1}{2}}} - 1\right\}. \tag{4.7}$$

The expressions for C_1 and C_2 do not have simple analytical solutions. The integrals can be expanded in a series for large and small values of μ, however a numerical technique was preferred. The integrands in equations (4.7) are very slowly varying functions of ξ' (for ξ' greater than a few airfoil chords) and

approach zero as ξ' approaches infinity. The integrands are harmonic functions requiring that $\mu\xi'$ be truncated at the end of a complete cycle. Hence $\mu\xi'$ must be an exact even multiple of π. Using this technique, it is found that a value of ξ' of about 10 chords gives a high degree of accuracy. The value of ζ' actually fluctuates around 10 chords as $\mu\xi'$ is kept as an exact even multiple of π. The integrals involving T_2, T_3 and T_4 have an infinite integrand at the lower limit of integration and care must be taken in numerically determining the Cauchy principal value. Using (2.4) and (4.2), integration of the pressure coefficient gives the lift coefficient as

$$C_{L0} = 2\left(\frac{b'+1}{2}\right)^2 \int_0^\pi \phi_0 \sin 2\theta \, d\theta - (1-b'^2) \int_0^\pi \phi_0 \sin\theta \, d\theta,$$

where C_{L0} is the amplitude of the non-steady lift coefficient such that

$$C_L = C_{L0}\, e^{j\omega t}, \quad \phi = \phi_0\, e^{j\omega t}.$$

The solution of this integral is

$$C_{L0} = -C_1 D_1 + C_2 D_2 - j\mu v_0 D_3,$$

where
$$D_1 = \pi\{[\tfrac{1}{2}(b'+1)]^2 [2\theta_1 \cos 2\theta_0 - \sin 2\theta_1] + (1-b'^2)[\sin\theta_1 - \theta_1 \cos\theta_0]\},$$
$$D_2 = \pi\{[\tfrac{1}{2}(b'+1)]^2 [2(\theta_1-\pi)\cos 2\theta_0 - \sin 2\theta_1] + (1-b'^2)[\sin\theta_1 - (\theta_1-\pi)\cos\theta_0]\}$$

and

$$D_3 = \frac{1}{2}\left(\frac{b'+1}{2}\right)^4 [\theta_1 + \tfrac{1}{4}\sin 4\theta_1] - \frac{3}{4}\left(\frac{b'+1}{2}\right)^2 (1-b'^2)[\sin\theta_1 + \tfrac{1}{3}\sin 3\theta_1] + \tfrac{1}{4}(1-b'^2)^2 [\theta_1 + \tfrac{1}{2}\sin 2\theta_1].$$

If the quasi-steady lift coefficient C_{Ls} is defined to be the value of the non-steady lift coefficient for μ approaching zero, then the ratio of the non-steady lift coefficient to the quasi-steady lift coefficient is

$$C_{L0}/C_{Ls} = Q(\mu) - j\mu D_3/D_1,$$

where
$$Q(\mu) = -\frac{C_1}{v_0} + \frac{C_2}{v_0}\frac{D_2}{D_1},$$

and the lift coefficient can be written as

$$C_L = v_0 D_1\, e^{j\omega t}\,[Q(\mu) - j\mu D_3/D_1]. \tag{4.8}$$

This lift coefficient can now be integrated over all frequencies to determine the unit step spoiler actuation solution.

4.4. *Unit step spoiler actuation*

The complete linearity of the blowing theory for $K = 0$ makes it possible to use the methods of superposition to obtain the transient spoiler actuation solution. The second term of (4.8) represents the contribution of the apparent mass term and will be discarded since it has no contribution to the solution. The remaining function $Q(\mu)$, shown in figure 9 for a particular airfoil configuration, becomes asymptotic to the negative imaginary axis. This indicates that the real part of

the lift approaches zero as μ approaches infinity. Physically it can be argued that the 'blowing' and 'sucking' cycles occur so rapidly that the wake circulation cancels the lift more effectively. The boundary condition on the spoiler for the unit step actuation is

$$v = (\sin\delta)\,1(t),$$

where $1(t)$ is the Heaviside integral. If v_0 is put equal to $(\sin\delta)/2\pi j\omega$ and (4.8) is integrated over all frequencies, the lift coefficient becomes

$$C_L = \sin\delta D_1 \frac{1}{2\pi j}\int_{-\infty}^{\infty} \frac{e^{j\omega t}}{\omega} Q(\mu)\,d\omega.$$

Suppose that

$$Ut = s'c,$$

where s' is the distance moved in chords, then the lift coefficient can be written as

$$C_L = C_{Lf} I(s'),$$

where C_{Lf} is the final steady-state lift coefficient,

$$I(s') = \frac{1}{2\pi j}\int_{-\infty}^{\infty} \frac{e^{jks'}}{k} Q(k)\,dk, \tag{4.9}$$

and the frequency parameter k is given by $k = \mu c$. The technique for solving this type of integral is given in detail by Bisplinghoff *et al.* (1955). Suppose that

$$Q(k) = R(k) + jS(k),$$

where R and S are real functions of k, then (4.9) becomes

$$I(s') = \frac{2}{\pi}\int_0^{\infty} \frac{R(k)\sin ks'}{k}\,dk. \tag{4.10}$$

$R(k)$ is only known numerically and therefore numerical techniques must be employed to solve this integral. $R(k)$ and the rate of change of $R(k)$ approach zero for increasing k. This and the k factor in the denominator make the integrand of this integral rapidly approach zero. Truncating the integrand at a length corresponding to an even multiple of π allows this integral to be solved accurately for k no greater than about 25.

4.5. *Finite time spoiler actuation*

In practical applications, spoiler actuation takes a finite period of time and it is desirable that this problem be included. The unit step integral (4.10) is entirely independent of the spoiler angle and this allows superposition of unit step solutions. Suppose the spoiler is erected to angle δ by N equal finite steps of $\Delta\delta$. During each step the airfoil travels $\Delta s'$ and at the completion of spoiler erection, the lift coefficient is

$$C_L = D_1\Delta\delta\{I_1[N\Delta s'] + I_2[(N-1)\Delta s'] + \ldots + I_{N+1}[0]\}.$$

If the airfoil travels a total distance s' which is greater than the distance s'_e travelled during spoiler erection, the lift coefficient is

$$C_L = D_1\Delta\delta\{I_1[s'] + I_2[s' - s'_e/N] + \ldots + I_{N+1}[s' - s'_e]\}.$$

For large N, $\Delta\delta/\delta \ll 1$ and $\Delta\delta$ can be replaced by $\delta/(N+1)$. This gives the final steady-state lift coefficient as

$$C_L = C_{Lf}\, W(s'), \tag{4.11}$$

where $$W(s') = \frac{1}{N+1}\{I_1[s'] + I_2[s' - s'_\varepsilon/N] + \ldots + I_{N+1}[s' - s'_\varepsilon]\}.$$

In (4.11), C_{Lf} should be $D_1\delta$ and not $D_1 \sin\delta$, however since it is the response function $W(s')$ that is the important part of this solution, it is allowable for conformity purposes to write the solution with C_{Lf} as determined in the steady-state case. Typically, $N = 20$ shows good results. With N chosen, the lift coefficient is a function of the total distance travelled and the distance travelled during spoiler erection.

5. Experiments

Measurements of steady lift, drag and pitching moment were taken for a 14 % thick Clark Y airfoil. It was constructed of wood and had a 14 in. chord. Each end of the airfoil had $\frac{1}{8}$ in. steel plates attached to allow spanwise spoilers of heights 5 and 10 % of the chord length to be mounted at different angles to the airfoil surface and at varying positions on the airfoil. Measurements were taken for spoiler positions 50% and 70 % along the chord, and at angles of 30°, 60° and 90°.

The airfoil was mounted at the mid-chord position on a six-component strain-gauge balance system. The lift, drag and pitching moment were measured over a wide range of incidence angles. The gap between the spoiler and the airfoil surface was sealed with masking tape for each configuration. The base pressure in the wake region was measured by taping a thin tube to the airfoil in the wake region. This tube was connected to an alcohol manometer, together with a tube leading to a static probe measuring the upstream undisturbed static pressure. The test Reynolds number was 4×10^5.

Similar measurements were taken on a 14 % thick Clark Y airfoil with a 32·5 % flap. For these measurements the airfoil was mounted at the $\frac{1}{4}$-chord point. The gap on the lower surface between the main foil and the flap was sealed with masking tape.

All measurements were made in the low-speed wind tunnel of the Mechanical Engineering Department of the University of British Columbia. This tunnel has a test section of 3 ft by $2\frac{1}{4}$ ft over a length of $8\frac{2}{3}$ ft. The tunnel produces a very uniform flow, with a turbulence level of less than 0·1 % over a wind speed range of 0–150 ft/s.

The wind-tunnel wall correction technique employed was the same as that employed by Jandali (1970). This method uses the corrections established by Pope & Harper (1966, §6.7), with a dimensionless wake blockage velocity increment of $\frac{1}{4}(c/H)C_D$ instead of $\frac{1}{2}(c/H)C_D$, where H is the tunnel wall spacing and C_D is the airfoil drag coefficient. Jandali found that measurements on airfoils of varying chord lengths collapsed better using these corrections. There exists some controversy over the techniques employed for correcting the wake pressure coefficient. Bluff-body and stalled-airfoil techniques such as those presented by

Maskell (1963) are not strictly applicable in this case. To overcome this problem, base pressure measurements were taken over a range of incidence angles on airfoils of chords 9, 14, 19 and 24 in. long for normal spoilers of 5 and 10 % height, located at both the 50 and 70 % chord positions. These measurements were plotted and interpolated back to zero-chord conditions (or infinite stream). The base pressure coefficients for the remaining spoiler angles, for which measurements were taken on the 14 in. chord airfoil, were then corrected in the same respective ratio. It is realized that, as the spoiler angle changes, the wake characteristics also change slightly. This in turn would affect the correction ratios slightly. This technique does, however, give reasonably realistic results and was used in the absence of better information.

At low airfoil incidence and small spoiler angle the possibility of flow reattachment occurs. In such a case the theory is not applicable. To ensure that measurements were not taken for such cases tufts of cotton were attached to the airfoil surface in the wake region. Observation of these tufts in all airfoil configurations was carefully carried out. The lower surface of the Clark Y airfoil is flat, and this base is used as a reference for incidence rather than the usual chord line.

The model used for transient loading measurements was also a 14 % thick Clark Y airfoil of 14 in. chord. However, it was made of steel and had a mid-span section instrumented with 24 pressure taps, each of which could be connected in sequence to a cavity containing a condenser microphone. A spoiler of 8·5 % chord height mounted at the 70 % chord position could be actuated at different constant rates to any angle up to 90° by a Slo-Syn motor.

For a given combination of wind speed, airfoil incidence, spoiler angle and actuation rate, the spoiler was actuated repeatedly with each pressure tap connected in turn to the microphone cavity. Each transient tap pressure was determined from a photograph of the microphone output on the screen of a storage oscilloscope, such as that of figure 3 (plate 1), taken for a tap near the nose of the airfoil. The instantaneous pressure distribution of the airfoil at any time after the start of spoiler actuation was determined from the ordinate of the trace on each photograph at that time, and the area of the pressure distribution was measured to determine the instantaneous lift.

6. Results and comparisons

In this section, the lift predicted by the theory for both the steady state and the transient state following spoiler actuation is compared with experimental results and, where possible, with the predictions of the theory of Woods (1953) as modified by Barnes (1965). Corrected experimental base pressure coefficients $-K$ used in the calculations ranged from $-0{\cdot}3$ to $-0{\cdot}65$, and corresponding calculated values of l ranged from 3·0 to 1·2.

6.1. *Steady-state lift*

In figure 4(*a*), the lift coefficient C_L is plotted as a function of the incidence angle α for a Clark Y airfoil of 14 % thickness with a normal 10 % spoiler at the 50 % chord position. The present theory is seen to give quite good agreement

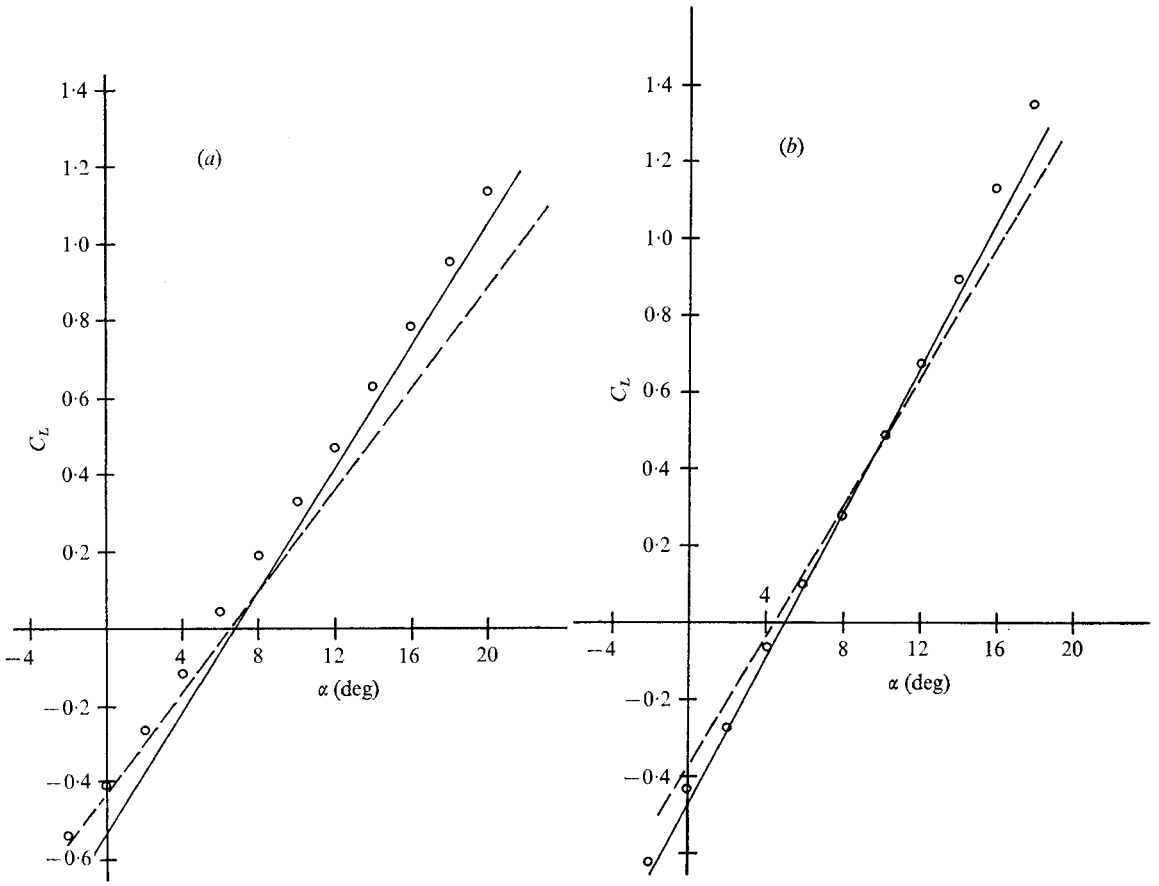

FIGURE 4. Lift *vs.* incidence angle for 14 % Clark Y airfoil with 10 % normal spoiler at (*a*) the 50 % and (*b*) the 70 % chord position. ——, present theory; — — —, Woods's (1953) theory; ○, experiments.

with the experimental results, particularly for positive C_L. Woods's theory gives better agreement for negative C_L, but worse agreement for positive C_L, and predicts too low a value of $dC_L/d\alpha$. In figure 4 (*b*), the configuration is the same except that the normal spoiler is at the 70 % chord position. Here the present theory gives excellent agreement with the experimental values. (The concave upward trend of the data at high C_L results from the growing bubble separation in front of the spoiler, not accounted for in the theory.) Woods's theory also gives quite good agreement, but again predicts too low a value of $dC_L/d\alpha$.

In figure 5 (*a*), the configuration is as in figure 4 (*b*), except that the normal spoiler is 5 % of the chord length in height. Both theories give good agreement with the experimental results, particularly Woods's theory, although the present theory gives a better value of $dC_L/d\alpha$. In figure 5 (*b*), values are shown for the same airfoil with a 10 % spoiler inclined at 60° to the surface at the 70 % chord position. The present theory is again seen to give good agreement with the experimental points. Woods's theory was not calculated for this case, since Barnes's empirical

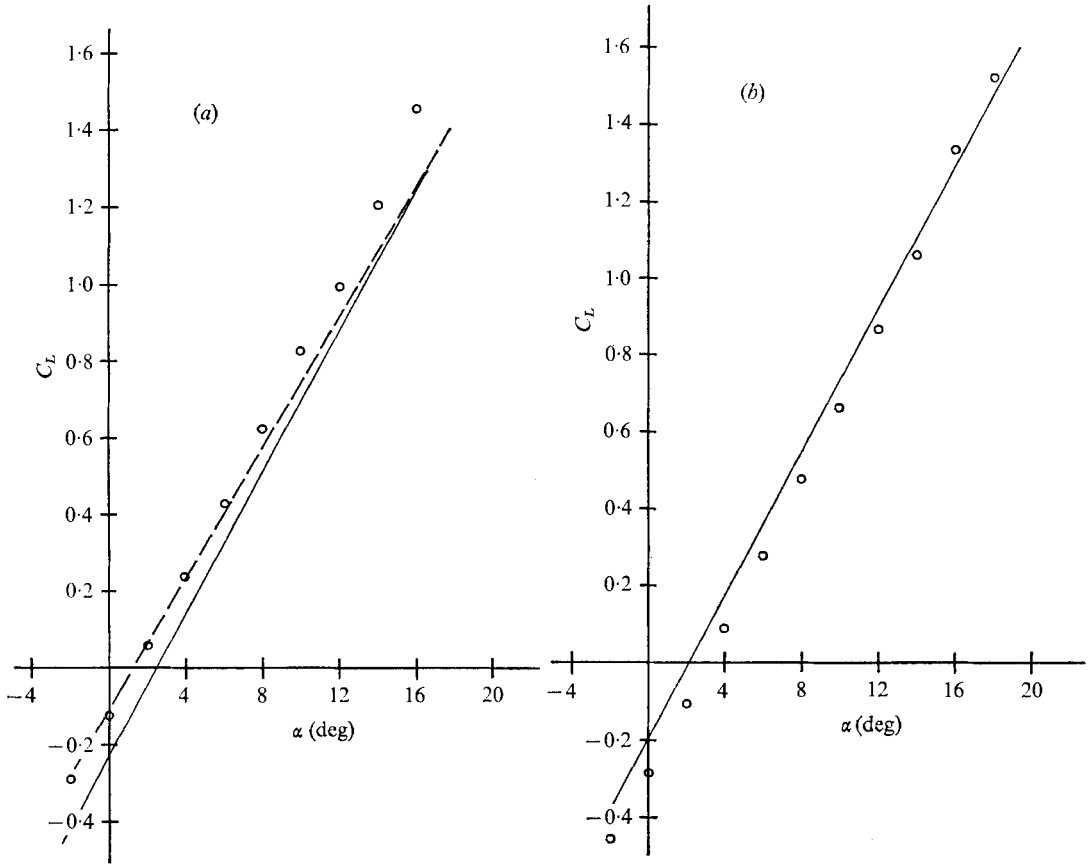

FIGURE 5. Lift *vs.* incidence angle for 14 % Clark Y airfoil with (*a*) 5 % normal spoiler and (*b*) 10 % spoiler inclined at 60° at the 70 % chord position. ——, present theory; — — —, Woods's (1953) theory; ○, experiments.

formula for the incremental pressure coefficient behind the spoiler, needed in the calculation, applies only to normal spoilers.

Figure 6 is a cross-plot at $\alpha = 6°$ for the same airfoil with a 10 % spoiler at the 70 % chord position, showing the dependence of C_L on spoiler angle δ. The present theory predicts the trend of the experimental values correctly, and gives respectable quantitative agreement. There are few published results of experiments on airfoil spoilers, so when some unpublished results of two-dimensional spoiler tests on one of their airfoils were made available to the authors by de Havilland, Canada, it seemed useful to make a comparison with the predictions of the present theory. This is shown in figure 7. The theory could not be calculated for the actual airfoil, since its co-ordinates were not available, so the theory was calculated for the 14 % thick Clark Y airfoil, and the comparison was made for the same spoiler geometry (8·2 % spoiler at the 69 % chord position) and at the same incidence measured from zero lift incidence for the basic airfoil (12·5°), to equalize the effects of camber. The theoretical curve is seen to agree quite closely with the experimental points. The agreement would have been closer still if the theory had been calculated for an airfoil of the thickness of the test airfoil (18 %).

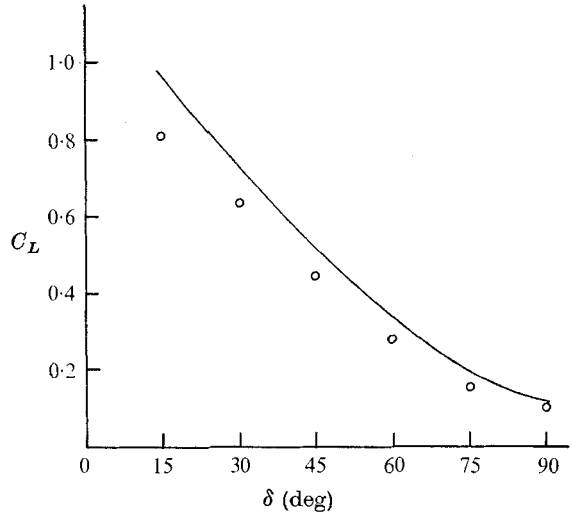

FIGURE 6. Lift *vs.* spoiler inclination for 14 % Clark Y airfoil at 6° incidence with 10 % spoiler at the 70 % chord position. ——, present theory; ○, experiments.

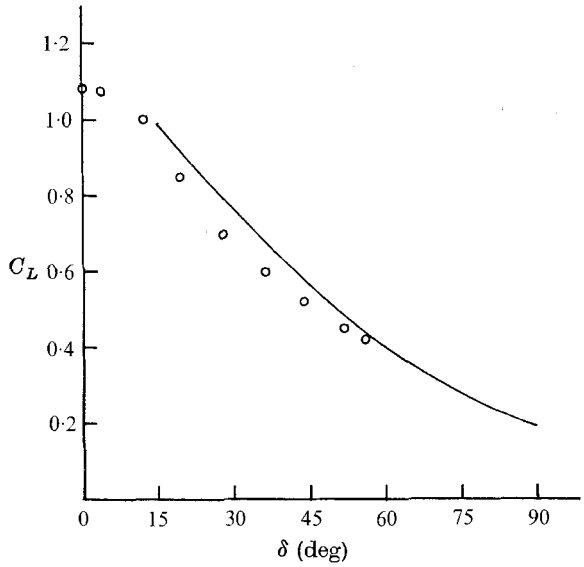

FIGURE 7. Lift *vs.* spoiler inclination for airfoil at 12·5° incidence (from zero lift) with 8·2 % spoiler at the 69 % chord position. ——, present theory, for 14 % Clark Y airfoil; ○, experiments (unpublished results for 18 % de Havilland Canada airfoil).

The final steady-state comparison, shown in figure 8, is for the 14 % Clark Y airfoil with a 10 % normal spoiler at the 70 % chord position, and with a simple flap 32·5 % of the chord length deflected by 15°. Woods's theory with Barnes's empirical modification can be calculated for this case, since the spoiler is normal, and the two theories are seen to give good agreement with the experimental points, the present theory being slightly the better.

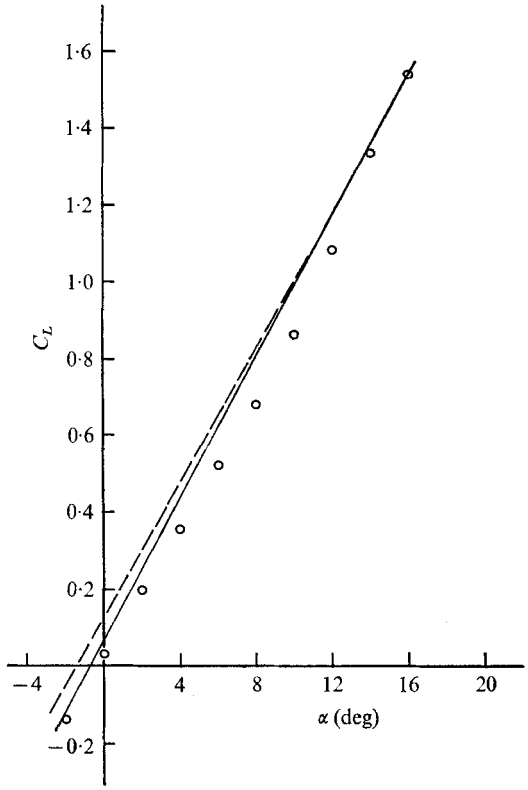

FIGURE 8. Lift *vs.* incidence angle for 14 % Clark Y airfoil with 10 % normal spoiler at the 70 % chord position, and simple flap at the 32·5 % chord position deflected by 15°. ——, present theory; – – – –, Woods's (1953) theory; ○, experiments.

6.2. *Transient lift*

As shown in § 4.4, the transient lift is obtained by an integral transform of the function $Q(\mu)$, which represents, except for the omission of the apparent-mass term, the ratio of instantaneous to quasi-steady lift in the 'blowing' theory. Figure 9 shows $Q(\mu)$ for the case corresponding to a 10 % spoiler at the 70 % chord position. The lift approaches the quasi-steady value, as expected, as the frequency parameter μ approaches zero, and the real part of the lift approaches zero for large μ. This may be argued in terms of the 'blowing' and 'sucking' cycles occurring so rapidly at large μ that the net effect approaches zero.

For the unit step and finite rate spoiler actuation problems, the results are reported as the ratio $W(s')$ of the instantaneous lift to the final steady-state lift as a function of airfoil travel s' in chords. Since this form of presentation eliminates the dependence on spoiler angle, the solution becomes a function of spoiler position and height only. Also, the lift given by $W(s')$ is that due to the spoiler actuation only, so if the complete instantaneous lift is wanted, the previous steady-state solutions for incidence, camber, thickness and flap must be added as required.

Figure 10 shows $W(s')$ calculated for a 10 % spoiler at the 70 % chord position

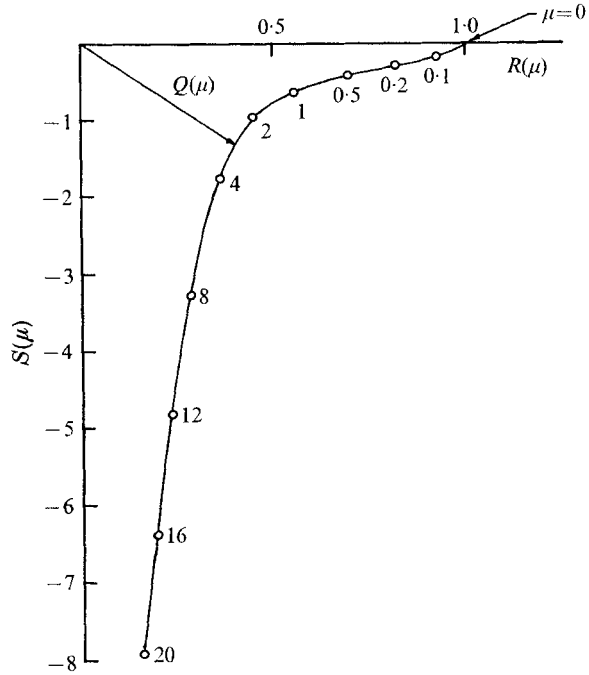

FIGURE 9. Lift function in 'blowing' theory, corresponding to 10 % spoiler at the 70 % chord position.

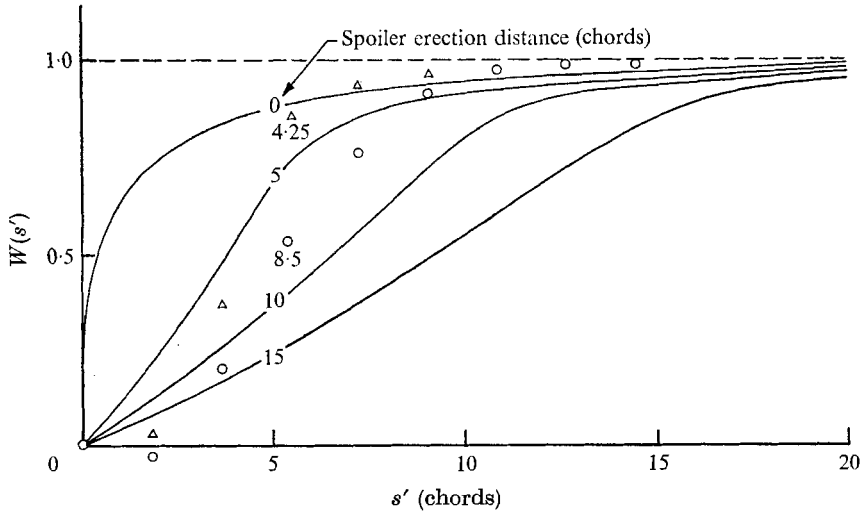

FIGURE 10. Transient lift decrement function for 10 % spoiler at the 70 % chord position. ——, present theory; ○, △, experiments on 14 % Clark Y airfoil.

for various values of the erection time in terms of airfoil travel, including the unit step. Two sets of measured values are also included. These represent erection of the spoiler to 45° and 90° at the same constant rate, giving airfoil travel during erection of 4·25 and 8·5 chords, respectively. The incidence angle was 12°. It would have been desirable to carry out more measurements, for different values

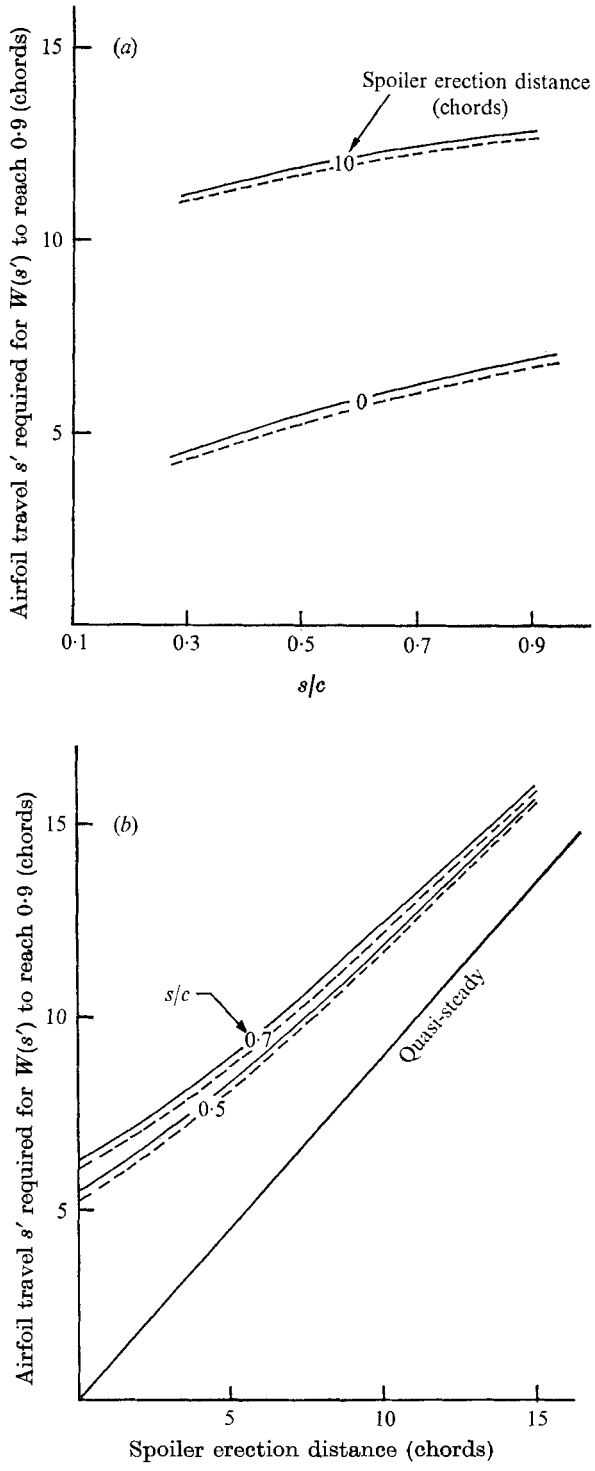

FIGURE 11. Effect of (*a*) spoiler position and (*b*) spoiler erection rate on transient lift by present theory. ——, 10% spoiler; – – –, 5% spoiler.

of α, δ and erection rate, but unfortunately the wind tunnel had to be dismantled after these two tests, for transfer to a new laboratory building, and further tests have been delayed. The meaning of $W(s')$ for the experimental values is slightly different. It is the ratio of the instantaneous decrement of lift due to spoiler actuation to the corresponding steady-state decrement from the basic airfoil lift. (In the theory, the sum of the lifts from the incidence, camber and thickness cases is not the basic airfoil lift, since the effect of the cavity is included in them.)

When these differences, and the fact that the high incidence case tested is not the most favourable for comparison with the theory, and the use of free-stream cavity pressure in the theory, are considered, the degree of agreement between theory and experiment in figure 10 can be considered at least promising, since the experimental points fall in about the right places between the theoretical curves, although the experimental increase of $W(s')$ is more abrupt.

Figures 11 (*a*) and (*b*) are summary plots of the effects predicted by the theory of different parameters on the time for the transient lift to reach 90 % of the steady-state value. In figure 11 (*a*), the effect of spoiler position is shown for 5 and 10 % spoilers in unit step and finite rate erection, and it is seen that the spoiler height has little effect (justifying the comparison of experimental data for an 8·5 % spoiler with theoretical results for a 10 % spoiler in figure 10), but that the time to reach 90 % of steady-state lift increases as the spoiler is moved towards the airfoil trailing edge. In figure 11 (*b*), the effect of the spoiler erection rate is shown for 5 and 10 % spoilers at the 50 and 70 % chord positions, and the common gradual trend towards the quasi-steady solution is evident.

7. Discussion

The present theory appears to give quite accurate predictions of the steady-state lift of airfoils with spoilers. The previous theory of Woods (1953), using Barnes's (1965) empirical formula for the incremental base pressure coefficient, also gives quite good predictions, but generally with too low a value of $dC_L/d\alpha$. This would be improved if another empirical recommendation of Barnes was incorporated in Woods's theory, the use of a reduced effective spoiler height as a function of the airfoil boundary-layer displacement thickness. This was not done here, to give a fair comparison of the two theories, since no effect of the boundary layer is incorporated in the present theory.

Woods's theory for C_L is simpler to use, requiring only slide-rule computations, whereas the present theory, with its series for the camber and thickness effects, requires a computer program for computation of C_L. However, Woods's theory requires empirical specifications of both the complete spoiler base pressure coefficient (to give the separation velocity from the spoiler tip) and the incremental base pressure coefficient caused by the spoiler. The latter is awkward to determine, and no formula for it is available for inclined spoilers, Barnes's formula applying only to normal spoilers. The present theory requires empirical specification of the spoiler base pressure coefficient only.

The theory can easily be extended to the calculation of the pitching moment, but so far this has not been done. Although the present steady-state theory

appears to provide some improvement over Woods's theory, the main reason for working it out was to provide a stepping stone to the transient theory. The agreement of this theory for transient lift following spoiler actuation with preliminary wind-tunnel measurements is encouraging, and it seems probable that the use of the free-stream cavity pressure in the calculation of the function $W(s')$ does not lead to serious error. It is hoped that the theory will be of use in the preliminary design of airfoils or hydrofoils with retractable spoilers.

The spoiler airfoil for transient measurements was designed by A. K. Dixit and the preliminary wind-tunnel tests of figure 10 were carried out by undergraduate students G. Wohlfarth and D. Bruce. Financial support was provided by the Defence Research Board of Canada under Grant 9551-13.

REFERENCES

BARNES, C. S. 1965 A developed theory of spoilers on aerofoils. *Aero Res. Counc. Current Paper*, no. 887.

BIOT, M. A. 1942 Some simplified methods in airfoil theory. *J. Aero. Sci.* **9** (5), 185.

BISPLINGHOFF, R. L., ASHLEY, H. & HALFMAN, R. L. 1955 *Aeroelasticity*, p. 284. Addison-Wesley.

BROWN, G. P. 1971 Steady and nonsteady potential flow methods for airfoils with spoilers. Ph.D. thesis, University of British Columbia.

FABULA, A. G. 1962 Thin-airfoil theory applied to hydrofoils with a single finite cavity and arbitrary free streamline detachment. *J. Fluid Mech.* **12**, 227.

HESS, J. L. & SMITH, A. M. O. 1966 Calculation of potential flow about arbitrary bodies. *Prog. Aero Sci.* **8**.

JANDALI, T. 1970 A potential flow theory for airfoil spoilers. Ph.D. thesis, University of British Columbia.

JANDALI, T. & PARKINSON, G. V. 1970 A potential flow theory for airfoil spoilers. *Trans. C.A.S.I.* **3** (1), 1.

MASKELL, E. C. 1963 A theory of blockage effects on bluff bodies and stalled wings in a closed wind tunnel. *Aero Res. Counc. R. & M.* no. 3400.

PARKIN, B. R. 1959 Linearized theory of cavity flow in two dimensions. *RAND Rep.* P-1745.

PARKINSON, G. V. & JANDALI, T. 1970 A wake source model for bluff body potential flow. *J. Fluid Mech.* **40**, 3, 577.

POPE, A. & HARPER, J. J. 1966 *Low-Speed Wind Tunnel Testing*. Wiley.

SONG, C. S. 1965 Supercavitating flat plate with an oscillating flap at zero cavitation number. *St Anthony Falls Hydraulic Lab. Tech. Paper*, B 52.

THEODORSEN, T. 1931 Theory of wing sections of arbitrary shape. *N.A.C.A. Rep.* no. 411.

WOODS, L. C. 1953 Theory of aerofoil spoilers. *Aero Res. Counc. R. & M.* no. 2969.

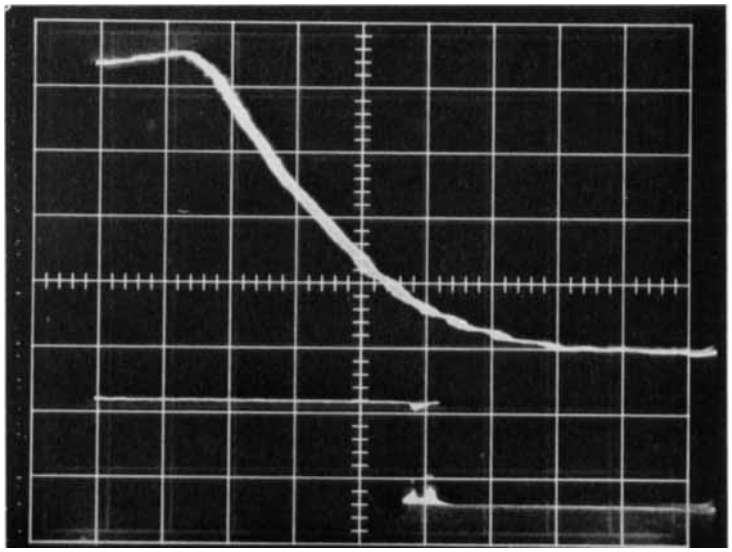

FIGURE 3. Upper trace: transient upper surface pressure near airfoil leading edge. Lower trace: trigger signal for start and finish of spoiler actuation.